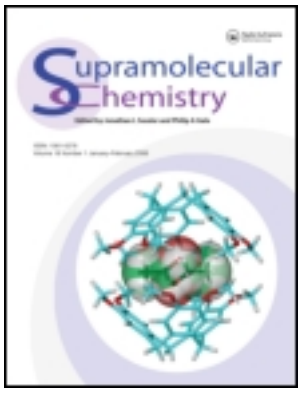

Supramolecular Chemistry
Publication details, including instructions for authors and subscription information:
http://www.tandfonline.com/loi/gsch20

Three-dimensional 3d-4f heterometallic coordination polymers: syntheses, structures and properties

Man-Sheng Chen [a b], Yue Zhao [a], Taka-Aki Okamura [c], Zhi Su [a], Wei-Yin Sun [a] & Norikazu Ueyama [c]

[a] Coordination Chemistry Institute, State Key Laboratory of Coordination Chemistry, School of Chemistry and Chemical Engineering, Nanjing National Laboratory of Microstructure, Nanjing University, Nanjing, 210093, P.R. China

[b] Department of Chemistry and Materials Science, Hengyang Normal University, Hengyang, 421008, P.R. China

[c] Department of Macromolecular Science, Graduate School of Science, Osaka University, Toyonaka, Osaka, 560-0043, Japan

Available online: 22 Feb 2011

To cite this article: Man-Sheng Chen, Yue Zhao, Taka-Aki Okamura, Zhi Su, Wei-Yin Sun & Norikazu Ueyama (2011): Three-dimensional 3d-4f heterometallic coordination polymers: syntheses, structures and properties, Supramolecular Chemistry, 23:01-02, 117-124

To link to this article: http://dx.doi.org/10.1080/10610278.2010.514908

Supramolecular Chemistry
Vol. 23, Nos. 1–2, January–February 2011, 117–124

Three-dimensional 3d-4f heterometallic coordination polymers: syntheses, structures and properties

Man-Sheng Chen[ab], Yue Zhao[a], Taka-Aki Okamura[c], Zhi Su[a], Wei-Yin Sun[a]* and Norikazu Ueyama[c]

[a]*Coordination Chemistry Institute, State Key Laboratory of Coordination Chemistry, School of Chemistry and Chemical Engineering, Nanjing National Laboratory of Microstructure, Nanjing University, Nanjing 210093, P.R. China;* [b]*Department of Chemistry and Materials Science, Hengyang Normal University, Hengyang 421008, P.R. China;* [c]*Department of Macromolecular Science, Graduate School of Science, Osaka University, Toyonaka, Osaka 560-0043, Japan*

(*Received 3 June 2010; final version received 24 July 2010*)

Six new 3d-4f heterometallic coordination polymers, $\{[Ln_4Cu_2(INAIP)_8(H_2O)_{15}]\cdot 14H_2O\}_n$ [Ln = La (**1**), Pr (**2**), Nd (**3**)] and $\{[LnCo_{0.5}(INAIP)_2(H_2O)_2]\cdot 2H_2O\}_n$ [Ln = Tb (**4**), Dy (**5**), Yb (**6**), H_2INAIP = 5-(isonicotinamido)isophthalic acid] have been synthesised and characterised by single crystal X-ray diffraction analysis. The results of structural analyses showed that **1**–**3** are isomorphous showing two-fold interpenetrated three-dimensional (3D) coordination framework, while **4**–**6** have the same non-interpenetrated 3D structure with 2D (4, 4) lanthanide-carboxylate layers. The results revealed that the different transition metal centres have great influence on the structures of the resulted complexes in this system. In addition, thermogravimetric and magnetic properties of **1**–**6**, and photoluminescence of **4** were investigated.

Keywords: heterometallic coordination polymers; magnetic property; photoluminescence property

Introduction

The rational design and synthesis of multidimensional metal-organic hybrid-extended frameworks are currently of great interest, which is justified not only by the fascinating structural diversity of the architectures but also by the potential applications of these compounds as functional materials (*1–8*). Furthermore, the synthesis and study of 3d-4f or 4d-4f heterometallic complexes are a challenge for chemists and have attracted increasing attention in last few years (*9–20*) because the competitive reaction containing 3d/4d-4f metal ions in conjunction with ligands may result in the formation of a mixture of homometallic assemblies rather than a heterometallic analogue. It has been reported that the lanthanide (4f) ions behave as hard acids and prefer to bind hard donors such as carboxylate oxygen, while d-block metal ions have a tendency to coordinate with N-donor ligands. Therefore, an appropriate approach towards the construction of 3d-4f or 4d-4f heterometallic frameworks is the reaction of a mixture of 3d or 4d and 4f metal salts with proper ligands containing both oxygen and nitrogen donors, such as nicotinic acid, pyridine-2,6-dicarboxylic acid and isonicotinic acid (*21–32*). Based on this approach, in this work, we use compound 5-(isonicotinamido)isophthalic acid (H_2INAIP) as a bridging ligand and potential linker between lanthanide(III) and transition metal(II) centres. Herein, we report the syntheses, crystal structures, luminescent and magnetic properties of two series of Ln(III)–M(II) complexes, namely $\{[Ln_4Cu_2(INAIP)_8(H_2O)_{15}]\cdot 14H_2O\}_n$ [Ln = La (**1**), Pr (**2**), Nd (**3**)] and $\{[LnCo_{0.5}(INAIP)_2(H_2O)_2]\cdot 2H_2O\}_n$ [Ln = Tb (**4**), Dy (**5**), Yb (**6**)].

Experimental

All commercially available solvents and starting materials were used as received without further purification. Ligand H_2INAIP was prepared as reported previously (*33*). FT-IR spectra were recorded on a Bruker Vector22 FT-IR spectrophotometer using KBr discs. Elemental analyses for C, H and N were taken on a Perkin-Elmer 240C elemental analyser at the Analysis Center of Nanjing University. The magnetic susceptibilities in the temperature range of 1.8–300 K were measured on a Quantum Design MPMS7 SQUID magnetometer in a field of 2000 Oe. Diamagnetic corrections were made with Pascal's constants for all samples. Thermogravimetric analyses (TGAs) were performed on a TGA V5.1A Dupont 2100 instrument heating from room temperature to 700°C under N_2 with a heating rate of 20°C/min. The luminescent spectra for the solid powdered samples were recorded at room temperature on an Aminco-Bowman Series 2 spectrophotometer with xenon arc lamp as the light source. In the measurements of the emission and excitation spectra, the pass width was 5.0 nm. All the measurements were carried out under the same conditions. Power X-ray diffraction patterns were

*Corresponding author. Email: sunwy@nju.edu.cn

ISSN 1061-0278 print/ISSN 1029-0478 online

DOI: 10.1080/10610278.2010.514908
http://www.informaworld.com

measured on a Shimadzu XRD-6000 X-ray diffractometer with Cu Kα ($\lambda = 1.5418$ Å) radiation at room temperature.

Preparation of {[$Ln_4Cu_2(INAIP)_8(H_2O)_{15}$]·$14H_2O$}$_n$ [Ln = La (1), Pr (2), Nd (3)]

A mixture of H_2INAIP (28.0 mg, 0.10 mmol), 0.05 mmol $Ln(NO_3)_3{\cdot}6H_2O$ [22.0 mg (**1**), 22.0 mg (**2**), 22.5 mg (**3**)], $Cu(OAc)_2{\cdot}H_2O$ (11.1 mg, 0.05 mmol), NaOH (8.0 mg, 0.20 mmol), H_2O (8 ml) was kept in a 15-ml Teflon liner autoclave at 140°C for 3 days. After the reaction mixture was cooled to room temperature, blue platelet crystals of the complex were collected. For **1**, yield: 23% based on La. Anal. calcd for $C_{112}H_{112}Cu_2N_{16}La_4O_{69}$: C, 38.63; H, 3.22; N, 6.44%. Found: C, 38.68; H, 3.29; N, 6.41%. IR (KBr pellet, cm^{-1}): 3440 (m), 1681 (s), 1612 (m), 1554 (s), 1432 (m), 1379 (s), 1281 (m), 890 (m), 784 (m), 734 (s), 668 (w), 599 (w). For **2**, yield: 16% based on Pr. Anal. calcd for $C_{112}H_{112}Cu_2N_{16}Pr_4O_{69}$: C, 38.54; H, 3.21; N, 6.42%. Found: C, 38.59; H, 3.27; N, 6.35%. IR (KBr pellet, cm^{-1}): 3441 (m), 1678 (s), 1611 (m), 1550 (s), 1432 (m), 1380 (s), 1282 (m), 890 (m), 786 (m), 774 (s), 669 (w), 599 (w). For **3**, yield: 15% based on Nd. Anal. calcd for $C_{112}H_{112}Cu_2N_{16}Nd_4O_{69}$: C, 38.39; H, 3.19; N, 6.39%. Found: C, 38.42; H, 3.24; N, 6.31%. IR (KBr pellet, cm^{-1}): 3445 (m), 1676 (s), 1617 (m), 1549 (s), 1427 (m), 1377 (s), 1287 (m), 888 (m), 788 (w), 788 (m), 719 (w), 598 (w).

Preparation of {[$LnCo_{0.5}(INAIP)_2(H_2O)_2$]·$2H_2O$}$_n$ [Ln = Tb (4), Dy (5), Yb (6)]

Complexes **4**–**6** were synthesised by the same procedure used for preparation of **1**–**3**, using 0.05 mmol $Ln(NO_3)_3{\cdot}6H_2O$ [23.0 mg (**4**), 23.5 mg (**5**), 25.1 mg (**6**)] and $Co(OAc)_2{\cdot}4H_2O$ (13.1 mg, 0.05 mmol). After cooling to room temperature, pink block crystals of complex were collected. For **4**, yield: 24% based on Tb. Anal. calcd for $C_{56}H_{48}CoN_8TbO_{28}$: C, 40.54; H, 2.89; N, 6.75%. Found: C, 40.64; H, 2.81; N, 6.79%. IR (KBr pellet, cm^{-1}): 3444 (s), 1677 (m), 1617 (m), 1548 (s), 1426 (m), 1376 (s), 1288 (m), 887 (w), 788 (w), 720 (m), 599 (w). For **5**, yield: 26% based on Dy. Anal. calcd for $C_{56}H_{48}CoN_8DyO_{28}$: C, 40.36; H, 2.88; N 6.73%. Found: C, 40.43; H, 2.82; N 6.81%. IR (KBr pellet, cm^{-1}): 3447 (s), 1675 (m), 1616 (m), 1549 (s), 1426 (m), 1376 (s), 1287 (m), 887 (w), 788 (w), 718 (m), 598 (w). For **6**, yield: 14% based on Yb. Anal. calcd for $C_{56}H_{48}CoN_8YbO_{28}$: C, 39.85; H, 2.84; N, 6.64%. Found: C, 39.89; H, 2.77; N, 6.71%. IR (KBr pellet, cm^{-1}): 3446 (s), 1677 (m), 1617 (m), 1549 (s), 1426 (m), 1376 (s), 1288 (m), 887 (w), 789 (w), 719 (m), 599 (w).

Crystal structure determination

Crystallographic data collections for complexes **1**–**3** were carried out on a Rigaku RAXIS-RAPID Imaging Plate diffractometer at 200 K, using graphite-monochromated Mo-Ka radiation ($\lambda = 0.71075$ Å). The structures were solved by direct methods using SHELXS-*97* (*34*) and expanded using Fourier techniques (*35*). All the non-hydrogen atoms were refined anisotropically on F^2 by full-matrix least-squares method. All the hydrogen atoms except those of water molecules were generated geometrically and refined isotropically using the riding model. Each disordered atom of O12, O13, O812 and O813 in **1** has the site occupancy factors of 0.5, while the ones of O751 and O753 have 0.469(12) and 0.531(12), O804 and O805 have 0.692(19) and 0.308(19) in **1**, respectively. O12, O14, O551, O553, O51, O51B, O815 and O816 in **2** disordered with site occupancy of 0.5, O813 and O814 have 0.26(2) and 0.74(2). In **3**, O11, O14, O813 and O814 have the site occupancy of 0.5, O51 and O51B have 0.508(11) and 0.492(11), O351, O353, O815 and O816 have the site occupancy of 0.49(7), 0.51(7), 0.29(3) and 0.71(3), respectively. Crystallographic data of **4**–**6** were collected at 293 K on a Bruker SMART CCD system equipped with graphite-monochromated Mo-Kα radiation ($\lambda = 0.71073$ Å) using the ω-φ scan technique. The data integration and empirical absorption corrections were carried out by SAINT programs (*36*). The structures were solved by direct methods using SHELXS-*97* (*34*). All the non-hydrogen atoms were refined anisotropically on F^2 by full-matrix least-squares technique (SHELXL-*97*) (*37*). All the hydrogen atoms except those of water molecules were generated geometrically and refined isotropically using the riding model, while those of water molecules in **4**–**6** were found directly. Details of the crystal parameters, data collection and refinements for **1**–**6** are summarised in Table 1. Selected bond lengths and angles for **1**–**6** are listed in Table S1. CCDC 779436, 779437, 779438, 779439, 779440 and 779441 contain the supplementary crystallographic data for **1**–**6**. These data can be obtained free of charge via http://www.ccdc.cam.ac.uk/conts/retrieving.html, or from the Cambridge Crystallographic Data Centre, 12 Union Road, Cambridge CB2 1EZ, UK; Fax (+44) 1223-336-033; or E-mail: deposit@ccdc.cam.ac.uk.

Results and discussion

Crystal structures of {[$Ln_4Cu_2(INAIP)_8(H_2O)_{15}$]·$14H_2O$}$_n$ [Ln = La (1), Pr (2), Nd (3)]

The results of X-ray diffraction analyses indicate that complexes **1**–**3** are isomorphous and have two-fold interpenetrated three-dimensional (3D) framework, accordingly, the structure of **1** is described representatively here in detail. The asymmetric unit of **1** contains three Cu(II) atoms, two of which locate on special positions, 4

Table 1. Crystallographic data for **1**–**6**.

Compound	**1**	**2**	**3**	**4**	**5**	**6**
Empirical formula	$C_{112}H_{112}Cu_2N_{16}La_4O_{69}$	$C_{112}H_{112}Cu_2N_{16}Pr_4O_{69}$	$C_{112}H_{112}Cu_2N_{16}Nd_4O_{69}$	$C_{56}H_{48}CoN_8TbO_{28}$	$C_{56}H_{48}CoN_8DyO_{28}$	$C_{56}H_{48}CoN_8Yb_2O_{28}$
Formula weight	3478.98	3486.98	3500.30	1657.79	1664.95	1686.03
Crystal system	Monoclinic	Monoclinic	Monoclinic	Triclinic	Triclinic	Triclinic
Space group	*C*2/c	*C*2/c	*C*2/c	$P\bar{1}$	$P\bar{1}$	$P\bar{1}$
a (Å)	42.547(4)	42.170(4)	42.077(4)	10.116(5)	10.1108(8)	10.0681(9)
b (Å)	21.881(2)	21.6921(18)	21.6748(14)	10.818(4)	10.8110(9)	10.7454(10)
c (Å)	34.290(3)	34.145(3)	34.094(3)	13.731(5)	13.7409(11)	13.7073(13)
α (°)	90.00	90.00	90.00	79.143(5)	79.1390(10)	79.161(2)
β (°)	126.021(4)	125.832(3)	125.700(3)	78.793(4)	78.7450(10)	78.8120(10)
γ (°)	90.00	90.00	90.00	86.296(5)	86.219(2)	86.568(2)
T (K)	200	200	200	293(2)	293(2)	293(2)
V (Å^3)	25,819(4)	25,323(4)	25,251(3)	1447.0(10)	1446.1(2)	1428.4(2)
Z	8	8	8	1	1	1
*D*c (g cm^{-3})	1.790	1.829	1.842	1.902	1.912	1.960
μ (mm^{-1})	1.731	1.955	2.062	2.802	2.943	3.637
F(000)	13,952	14,016	14,048	821	823	831
Data collected	97,594	104,054	113,491	7279	7354	7124
Independent data	22,702	28,955	28,777	5022	5115	4941
R_{int}	0.1641	0.1429	0.1478	0.0458	0.0240	0.0701
Parameters refined	1867	1875	1877	430	430	430
Goodness-of-fit	1.055	1.060	1.077	0.994	1.018	1.062
R_1 [$I > 2\sigma(I)$]	0.0655	0.0619	0.0612	0.0343	0.0332	0.0469
wR_2 [$I > 2\sigma(I)$]	0.1511	0.1373	0.1376	0.0853	0.0813	0.1214
R_1 (all data)[a]	0.1017	0.0989	0.0999	0.0372	0.0350	0.0482
wR_2 (all data)[b]	0.1712	0.1536	0.1555	0.0868	0.0821	0.1229

[a] $R_1 = \Sigma||F_o|-|F_c||/\Sigma|F_o|$.

[b] $wR_2 = |\Sigma w(|F_o|^2-|F_c|^2)|/\Sigma|w(F_o)^2|^{1/2}$, where $w = 1/[\sigma^2(F_o^2) + (aP)^2 + bP]$. $P = (F_o^2 + 2F_c^2)/3$.

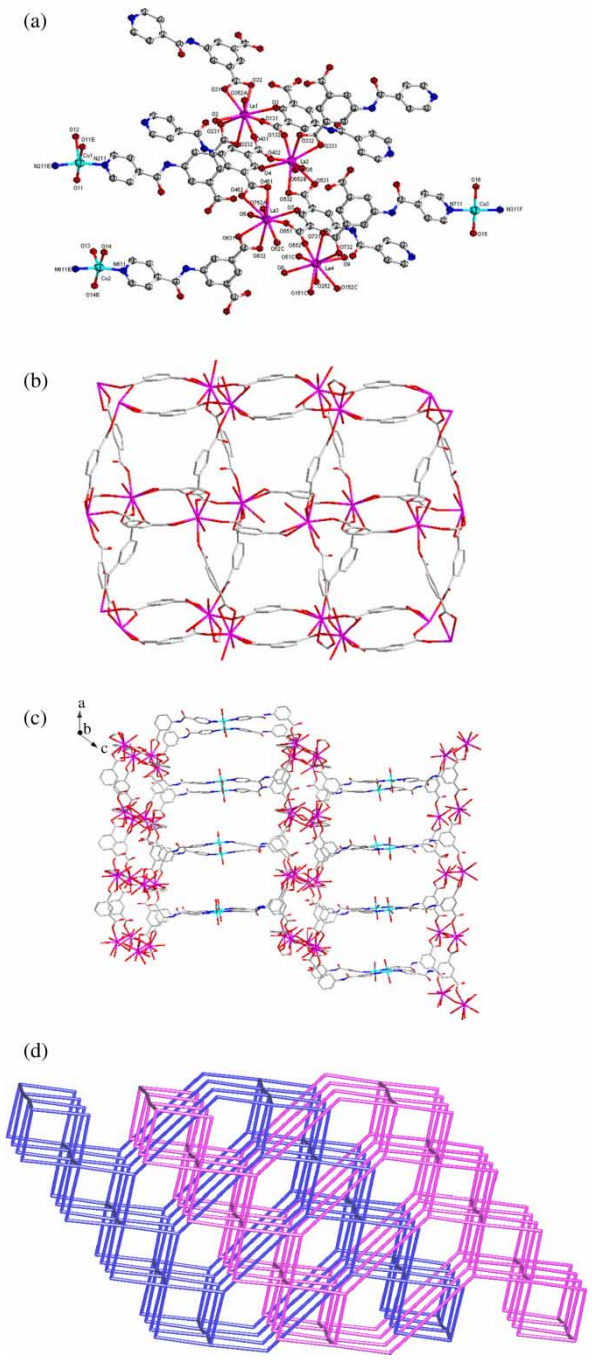

Figure 1. (a) Coordination environment of La(III) and Cu(II) in **1** with the ellipsoids drawn at the 30% probability level; hydrogen atoms and free water molecules were omitted for clarity. (b) 2D network constructed by La(III) and benzenedicarboxylate. (c) Perspective view of the 3D pillared structure of **1** with the uncoordinated pyridyl groups omitted for clarity. (d) Topological representation of the two-fold interpenetrated net in **1**.

La(III), 8 $INAIP^{2-}$ ligands, 15 coordinated (Figure 1(a)) and 14 non-coordinated water molecules. Cu1 and Cu2 have similar N_2O_3 coordination environment with distorted square-pyramidal coordination geometry, while Cu3 has slightly distorted square planar one. For example, Cu1 involves a N_2O_2 equatorial plane comprising two oxygen atoms from two coordinated water molecules and two nitrogen atoms from two $INAIP^{2-}$ ligands with normal Cu—O and Cu—N bond lengths varying from 1.967(6) to 2.010(6) Å (Table S1), and an axial position occupied by another coordinated water molecule with Cu—O bond length of 2.356(10) Å which is longer than those in equatorial plane due to the Jahn–Teller effect of Cu(II). On the other hand, each La(III) atom is nine-coordinated with distorted tricapped trigonal prism coordination geometry by seven carboxylate oxygen atoms from five different $INAIP^{2-}$ ligands and two ones from two terminal coordinated water molecules. The La—O bond distances in **1** range from 2.1086(16) to 2.1924(16) Å and the coordination angles around La(III) vary from 84.47(6)° to 174.62(6)° as listed in Table S1. It is interesting that the $INAIP^{2-}$ ligands in **1** exhibit two different kinds of coordination modes: one is connecting two La(III) by the carboxylate groups with coordination modes of μ_1-η^1:η^1-chelate and μ_1-η^1:η^0 monodentate and one Cu(II) through the pyridyl group, while the other one is coordinated to three La(III) through two carboxylate groups with coordination modes of μ_1-η^1:η^1-chelate and μ_2-η^1:η^1 bis-monodentate and the pyridyl group is free of coordination.

If the coordination interactions between the pyridyl group and Cu(II) as well as the Cu—O (water) one are neglected, a 2D double-layered network is formed by the La(III)–carboxylate coordination as shown in Figure 1(b). If the binuclear $La_2(OCO)_2$ subunits are considered as nodes, the 2D network can be regarded as a typical (4, 4) net. Such 2D (4, 4) nets are further connected together via the Cu—N coordination to generate a 3D pillared framework as illustrated in Figure 1(c). In order to minimise the hollow cavities and stabilise the framework, the potential voids formed via a single 3D framework show combination with another identical one, leading to the formation of a two-fold interpenetrated structure of **1** (Figure S1).

In order to better identify the nature of the 3D framework of **1**, suitable nodes and connectors can be defined using topological approach (*38–40*). As discussed above, the $INAIP^{2-}$ ligands link two La(III) atoms belonging to two different binuclear [La_2] units and one Cu(II) atom and thus can be defined as three-connectors, while the ones connecting three La(III) atoms can be regarded as two-connectors because these three La(III) belong to two different binuclear [La_2] units. On the other hand, each binuclear [La_2] unit links six $INAIP^{2-}$ ligands, and can be regarded as a six-connecting node, while each Cu(II) atom acts as a two-connecting node because it connects two $INAIP^{2-}$ ligands. The resulting structure of **1** is 3,6-c **sqc27** (http://epinet.anu.edu.au/sqc27) net with

stoichiometry (3-c)2(6-c), 2-nodal net Point (Schläfli) symbol for net: $(4{\cdot}6^2)_2(4^2{\cdot}6^{10}{\cdot}8^3)$ (Figure 2(d)) calculated by TOPOS (*40*).

Crystal structures of {[LnCo$_{0.5}$(INAIP)$_2$(H$_2$O)$_2$]·2H$_2$O}$_n$ [Ln = Tb (4), Dy (5), Yb (6)]

When $Co(OAc)_2{\cdot}4H_2O$, instead of $Cu(OAc)_2{\cdot}H_2O$, was used to react with ligand H_2INAIP in the presence of $Ln(NO_3)_3{\cdot}6H_2O$, complexes **4**–**6** with different structures from those of **1**–**3** were obtained. The results of X-ray crystallographic analysis revealed that **4**–**6** crystallise in the same triclinic space group $P\bar{1}$ and are also isomorphous. Therefore, complex **5** is taken as an example to describe its structure here. The asymmetric unit of **5** consists of one Dy(III) atom, one Co(II) atom sitting on an inversion centre, two $INAIP^{2-}$ ligands, two coordinated (Figure 2(a)) and two non-coordinated water molecules. Different from the four- and five-coordinated Cu(II) atoms in **1**, each Co(II) atom in **5** is six-coordinated with octahedral coordination geometry by two pyridyl nitrogen (N1B and N1C) and two carboxylate oxygen (O1 and O1A) atoms from four distinct $INAIP^{2-}$ ligands and two oxygen atoms (O1W and O1WA) from two water molecules with Co1—N bond length of 2.151(4) Å, the Co1—O ones are in the range of 2.090(3)–2.179(3) Å and bond angles around the Co(II) atom in the range of 87.43(13)°–180.0° (Table S1). The Dy1 in **5** is eight-coordinated, rather than nine-coordinated La in **1** (Figure 1(a)), with bicapped trigonal prism coordination geometry by seven carboxylate oxygen atoms from four $INAIP^{2-}$ ligands and one from a coordinated water molecule (Figure 2(a)). It is noteworthy that two unique $INAIP^{2-}$ ligands in **5** exhibit two different kinds of coordination modes: one coordinated to two Dy(III) and one Co(II) atoms using its two carboxylate groups with μ_1-η^1:η^1-chelate and μ_2-η^1:η^1 bis-monodentate coordination modes while the pyridyl group is free of coordination, the other one coordinated to two Dy(III) through the carboxylate groups with μ_1-η^1:η^1-chelate coordination mode and one Co(II) via the pyridyl group. When the Co—N and Co—O connections are neglected, a (4, 4) 2D network is formed by Dy(III)-carboxylate groups as shown in Figure 2(b), which is obviously different from that observed in **1** (Figure 1(b)). Then the 2D networks are further linked together by Co—N and Co—O coordination interactions to form a non-interpenetrated 3D framework (Figure 2(c)), rather than the two-fold interpenetrated 3D one of **1** (Figure S1). The different structures of **1**–**3** and **4**–**6** imply that the different transition metal centres play a crucial role in the formation of the ultimate 3D frameworks.

A similar topological method was used to get insight into the structure of **5**. According to the structural analysis,

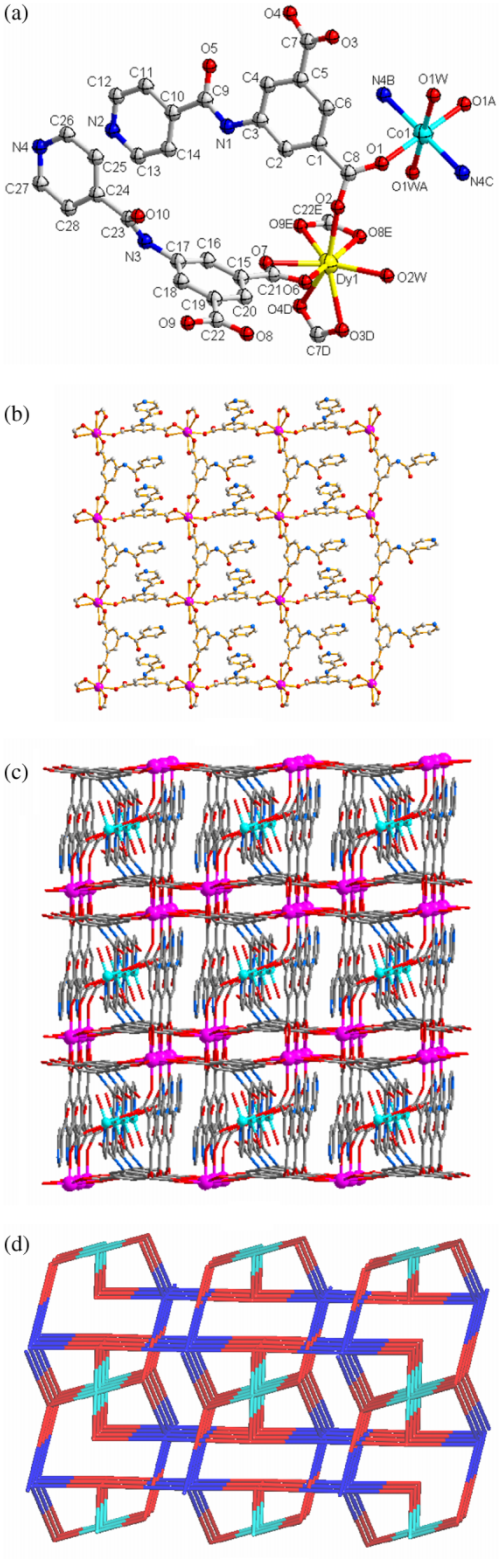

Figure 2. (a) Coordination environment of **5** with the ellipsoids drawn at the 30% probability levelhydrogen atoms and free water molecules were omitted for clarity. (b) 2D network in **5**. (c) View of the 3D framework of **5** all hydrogen atoms were omitted for clarity. (d) Topological representation of the 3D structure of **5**.

each $INAIP^{2-}$ ligand links three metal atoms and can be regarded as three-connector, and each Dy(III) as well as Co(II) links four $INAIP^{2-}$ ligands, thus both Dy(III) and Co(II) can be regarded as four-connecting nodes. Therefore, the final topology of **5**, calculated by TOPOS (*40*), is a 3,3,4-c net with stoichiometry (3-c)4(4-c)(4-c)2, 3-nodal net Point (Schläfli) symbol for net: $(8^3)_4(8^4{\cdot}10^2)(8^6)_2$, as shown in Figure 2(d).

Magnetic properties of complexes 1–6

As described above, in complexes **1**–**3**, the Cu(II) atoms are linked by pyridyl groups and the shortest Cu···Cu and Cu···Ln separations are 9.9925(18) and 12.6760(14) Å in **1**, 10.7953(18) and 12.6509(13) Å in **2**, and 10.7888(19) and 12.3480(16) Å in **3**, respectively, indicating that there are no interactions between Cu···Cu as well as between Cu···Ln. The temperature dependence of magnetic susceptibilities of **1**–**3** was measured in the range of 300–1.8 K with an applied magnetic field of 2000 Oe. As the temperature is lowered from room temperature to 1.8 K, the $\chi_M T$ value of **1** is almost constant (*ca.* 0.90 emu K mol^{-1}), which is close to the spin-only value of 0.907 emu K mol^{-1} based on two isolated Cu(II) ions in the unit, and the lanthanide ion La(III) is diamagnetic, indicating the basic paramagnetic property of **1** (Figure 3(a)). Taking into account the formula of **2**, the magnetic property can be given for a Pr_4Cu_2 unit, and the $\chi_M T$ and χ_M^{-1} (inset) vs. T plots (χ_M is the molar magnetic susceptibility for the Pr_4Cu_2 entity) are shown in Figure 3(b). The value of $\chi_M T$ at 300 K is 7.61 emu K mol^{-1}, which is slightly larger than the value expected for four magnetically quasi-isolated Pr(III) ions (4×1.60 emu K mol^{-1}) (*41*, *42*) plus two isolated Cu(II) ions (*ca.* 0.90 emu K mol^{-1}), namely 7.30 emu K mol^{-1}. The value of 1.60 emu K mol^{-1} for a Pr(III)-free ion ($g = 8/11$) can change in a given complex, but the variation should be small, owing to the character of the f^n complexes (*41*). The $\chi_M T$ values monotonically decrease to 1.45 emu K mol^{-1} at 1.8 K. It was found that the χ_M^{-1} *vs.* T plot follows the Curie–Weiss law above 50 K and gives the results: $C = 2.19$ emu K mol^{-1}, $\theta = -1.69$ K for **2** (Figure 3(b), inset). The characteristic of complex **3** is similar to that of **2**, and the $\chi_M T$ vs. T plot is shown in Figure 3(c). The feature of **2** and **3** may imply antiferromagnetic character, but as suggested by Kahn (*41*), for elements Pr(III) (f^2) and Nd(III) (f^3), the deviation from the Curie law is not necessarily an indication of ferro- or antiferromagnetic interactions. Similar to **2** and **3**, the temperature dependence of the magnetic susceptibilities of **4**–**6** was also measured in the temperature range ssof 1.8–300 K and the results are given in Figure S2. It was found that the χ_M^{-1} *vs.* T plots follow the Curie–Weiss law and give the results: $C = 17.67$ emu K mol^{-1}, $\theta = -16.34$ K for **4**; $C = 18.28$ emu K mol^{-1}, $\theta = -16.53$ K for **5**; $C = 4.24$ emu K mol^{-1}, $\theta = -3.74$ K for **6**, Despite the decrease in

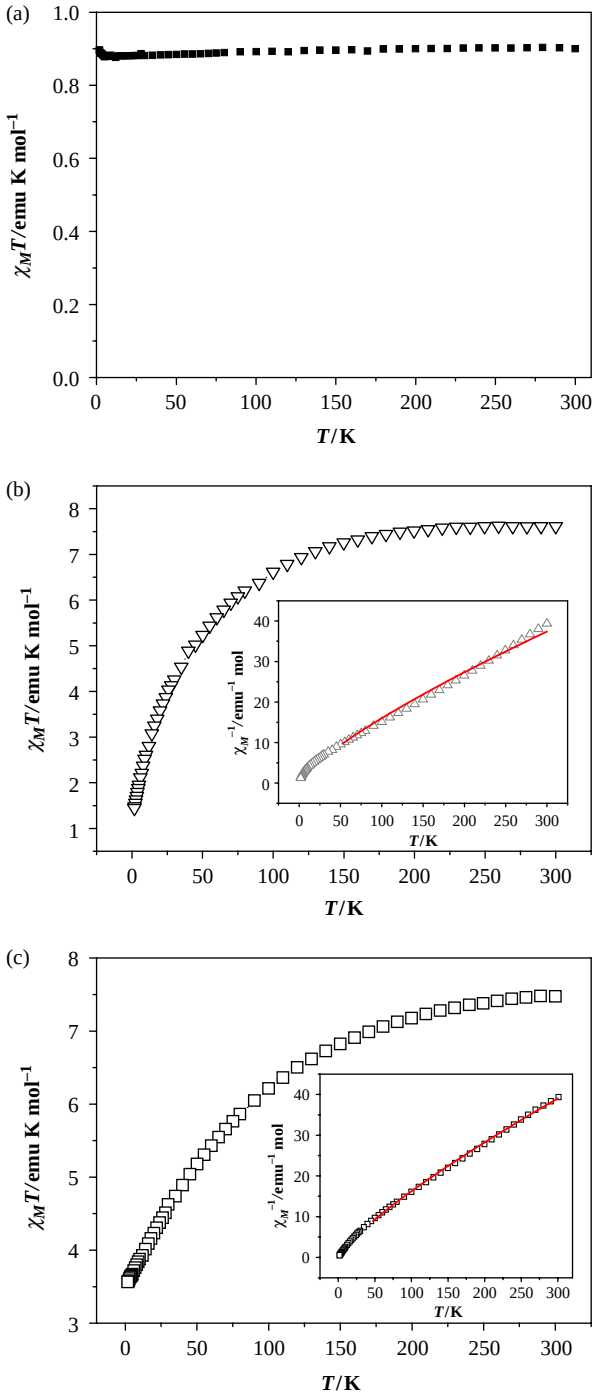

Figure 3. The $\chi_M T$ *vs.* T plots for (a) **1**, (b) **2** and (c) **3** (inset: χ_M^{-1} *vs.* T).

$\chi_M T$ value on cooling and the presence of negative θ value, the nature of the magnetic interaction between Ln(III) and Co(II) ions cannot be unambiguously interpreted as antiferromagnetic due to the strong spin-orbit coupling of the Ln(III) and Co(II) ions (*43*–*45*). On the other hand, the Ln···Ln distances range from 10.0681(9) to 10.818(4) Å in complexes **4**–**6**, the coupling interactions between

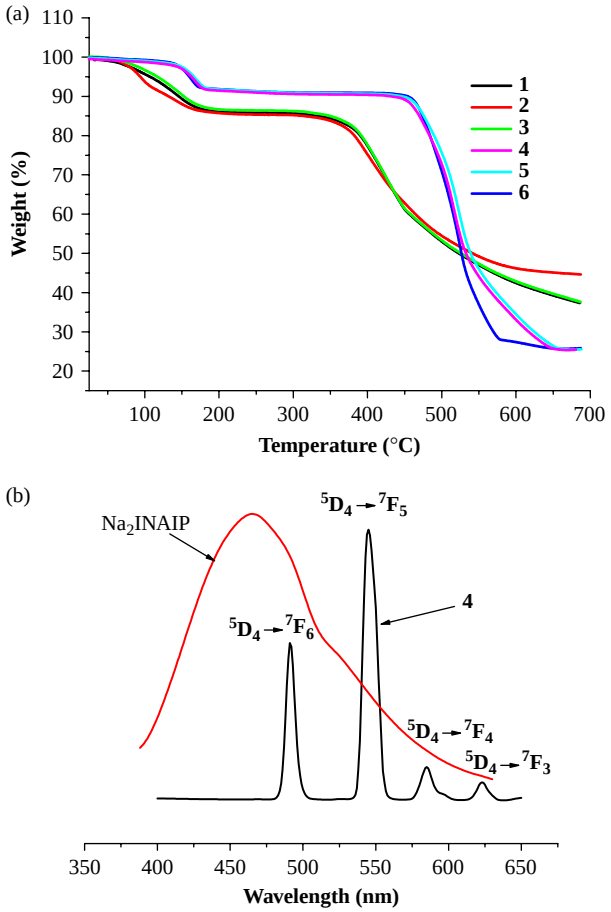

Figure 4. (a) The TG curves of compounds **1**–**6**. (b) The emission spectra of **4** and Na_2INAIP.

lanthanide ions bridged by $INAIP^{2-}$ ligands can be neglected. Therefore, we could not conclude the existence of antiferromagnetic coupling between adjacent lanthanide ions and/or Ln(III)–M(II) ions in **2**–**6** on the consideration of their strong spin-orbital coupling as well as the decrease in $\chi_M T$ may be due to the thermal depopulation of Stark sublevels together with crystal-field affection.

TGA and photoluminescence property of the complexes

As discussed above, compounds **1**–**3** and **4**–**6** are isomorphous, respectively, thus we choose compounds **1** and **5** to do PXRD for checking their phase purity, in which the experimental patterns are consistent with the simulated ones (Figure S3). The TGAs of compounds **1**–**6** were performed and the results are exhibited in Figure 4(a). The TGA data of **1** exhibit weight loss of 14.07% from 25 to 190°C, which corresponds to the loss of free and coordinated water molecules (calcd 15.04%). And then the residue began to decompose from *ca.* 340°C upon further heating. For complex **5**, the first weight loss of 8.35% between 25 and 190°C indicates the loss of free and coordinated water molecules (calcd 8.64%), and the residue remains unchanged until about 420°C. The other complexes showed similar TG behaviour.

Due to the excellent luminescent property of Tb(III), the photoluminescence properties for **4** and Na_2INAIP were investigated in the solid state at room temperature. The emission spectrum of **4** (Figure 4(b)) upon excitation at 330 nm exhibits the characteristic transitions of $^5D_4 \rightarrow {}^7F_J$ ($J = 6, 5, 4, 3$) of Tb(III). The peak at 545 nm is the strongest, ascribing to the $^5D_4 \rightarrow {}^7F_5$ transition which gave intense green luminescence output for **4**, while the intense emission band for Na_2INAIP ligand was observed at 465 nm ($\lambda_{ex} = 390$ nm).

Conclusions

In conclusion, we have successfully synthesised two series of novel 3D heterometallic coordination polymers with ligand 5-(isonicotinamido)isophthalic acid by hydrothermal methods. The structural difference between **1**–**3** and **4**–**6** implies that the different transition metal centres have great influence on the structure of the complexes in this system. The successful preparation of these complexes not only implies that the $INAIP^{2-}$ with N- and O-donors is a versatile ligand and useful for construction of 3d-4f hetero-metal-organic frameworks but also may provide valuable information for further construction of other 3d-4f frameworks.

Acknowledgements

This work was financially supported by the National Natural Science Foundation of China (Grant Nos 20731004 and 20721002) and the National Basic Research Program of China (Grant Nos 2007CB925103 and 2010CB923303).

References

(1) Cote, A.P.; Benin, A.I.; Ockwig, N.W.; O'Keeffe, M.; Matzger, A.J.; Yaghi, O.M. *Science* **2005**, *310*, 1166–1170.
(2) Yaghi, O.M.; O'Keeffe, M.; Ockwig, N.W.; Chae, H.K.; Eddaoudi, M.; Kim, J. *Nature* **2003**, *423*, 705–714.
(3) Wu, C.D.; Hu, A.; Zhang, L.; Lin, W.B. *J. Am. Chem. Soc.* **2005**, *127*, 8940–8941.
(4) Fang, Q.R.; Zhu, G.S.; Xue, M.; Wang, Z.P.; Sun, J.Y.; Qiu, S.L. *Cryst. Growth Des.* **2008**, *8*, 319–329.
(5) Koh, K.; Wong-Foy, A.G.; Matzger, A.J. *Angew. Chem., Int. Ed.* **2008**, *47*, 677–680.
(6) Blake, A.J.; Champness, N.R.; Hubberstey, P.; Li, W.S.; Withersby, M.A.; Schröder, M. *Coord. Chem. Rev.* **1999**, *183*, 117–138.
(7) Jiang, H.L.; Liu, B.; Akita, T.; Haruta, M.; Sakurai, H.; Xu, Q. *J. Am. Chem. Soc.* **2009**, *131*, 11302–13303.
(8) Jiang, H.L.; Tatsu, Y.; Lu, Z.H.; Xu, Q. *J. Am. Chem. Soc.* **2010**, *132*, 5586–5587.
(9) Liang, Y.C.; Cao, R.; Su, W.P.; Hong, M.C.; Zhang, W.J. *Angew. Chem. Int. Ed.* **2000**, *39*, 3304–3307.

(10) Chen, W.; Yuan, H.M.; Wang, J.Y.; Liu, Z.Y.; Yang, M.Y.; Chen, J.S. *J. Am. Chem. Soc.* **2003**, *125*, 9266–9267.
(11) Yu, Z.T.; Liao, Z.L.; Jiang, Y.S.; Li, G.H.; Li, G.D.; Chen, J.S. *Chem. Commun.* **2004**, 1814–1815.
(12) Zhao, B.; Cheng, P.; Dai, Y.; Cheng, C.; Liao, D.Z.; Yan, S.P.; Jiang, Z.H.; Wang, G.L. *Angew. Chem., Int. Ed.* **2003**, *42*, 934–936.
(13) Zhao, B.; Cheng, P.; Chen, X.Y.; Cheng, C.; Shi, W.; Liao, D.Z.; Yan, S.P.; Jiang, Z.H. *J. Am. Chem. Soc.* **2004**, *126*, 3012–3013.
(14) Zhao, B.; Chen, X.Y.; Cheng, P.; Liao, D.Z.; Yan, S.P.; Jiang, Z.H. *J. Am. Chem. Soc.* **2004**, *126*, 15394–15395.
(15) Blasse, G. *Mater. Chem. Phys.* **1992**, *31*, 3.
(16) Deng, H.; Shore, S.G. *J. Am. Chem. Soc.* **1991**, *113*, 8538–8540.
(17) Deng, H.; Chun, S.; Florian, P.; Grandinetti, P.J.; Sore, S.G. *Inorg. Chem.* **1996**, *35*, 3891–3896.
(18) Wan, Y.X.; Gu, X.J.; Xue, D.F. *J. Cryst. Growth* **2009**, *311*, 601.
(19) Bünzli, J.C.G. *Acc. Chem. Res.* **2006**, *39*, 53–61.
(20) Prasad, T.K.; Rajasekharan, M.V.; Costes, J.P. *Angew. Chem. Int. Ed.* **2007**, *46*, 2851–2854.
(21) Cai, Y.P.; Su, C.Y.; Li, G.B.; Mao, Z.W.; Zhang, C.; Xu, A.W.; Kang, B.S. *Inorg. Chim. Acta* **2005**, *358*, 1298.
(22) Liu, F.C.; Zeng, Y.F.; Jiao, J.; Li, J.R.; Bu, X.H.; Ribas, J.; Batten, S.R. *Inorg. Chem.* **2006**, *45*, 6129–6131.
(23) Song, Y.S.; Yan, B.; Weng, L.H. *Inorg. Chem. Commun.* **2006**, *9*, 567.
(24) Zhou, Y.F.; Jiang, F.L.; Yuan, D.Q.; Wu, B.L.; Wang, R.H.; Lin, Z.Z.; Hong, M.C. *Angew. Chem. Int. Ed.* **2004**, *43*, 5665–5668.
(25) Zhou, Y.F.; Hong, M.C.; Wu, X.T. *Chem. Commun.* **2006**, 135–143.
(26) Cutland-Van Noord, A.D.; Kampf, J.W.; Pecoraro, V.L. *Angew. Chem. Int. Ed.* **2002**, *41*, 4668–4670.
(27) Zaleski, C.M.; Depperman, E.C.; Kampf, J.W.; Kirk, M.L.; Pecoraro, V.L. *Angew. Chem. Int. Ed.* **2004**, *43*, 3912–3914.
(28) Gu, X.J.; Xue, D.F. *Inorg. Chem.* **2006**, *45*, 9257–9261.
(29) Gu, X.J.; Xue, D.F. *Cryst. Growth Des.* **2006**, *6*, 2551–2557.
(30) He, F.; Tong, M.L.; Chen, X.M. *Inorg. Chem.* **2005**, *44*, 8285–8292.
(31) Huang, Y.G.; Wang, X.T.; Jiang, F.L.; Gao, S.; Wu, M.Y.; Gao, Q.; Wei, W.; Hong, M.C. *Chem.-Eur. J.* **2008**, *14*, 10340–10347.
(32) Bai, Y.Y.; Huang, Y.; Yan, B.; Song, Y.S.; Weng, L.H. *Inorg. Chem. Commun.* **2008**, *11*, 1030–1032.
(33) Chen, M.S.; Bai, Z.S.; Okamura, T.-A.; Su, Z.; Chen, S.S.; Sun, W.Y.; Ueyama, N. *CrystEngComm* **2010**, *12*, 1935–1944.
(34) Sheldrick, G.M. *SHELXS-97, Program for the Solution of Crystal Structures*; University of Göttingen: Göttingen, Germany, 1997.
(35) DIRFID 99, Beurskens, P.T.; Admiraal, G.; Beurskens, G.; Bosman, W.P.; de Gelder, R.; Israel, R.; Smits, J.M.M. *The DIRFID-99 Program System*; Technical Report of the Crystallography Laboratory; University of Nijmegen: Nijmegen, The Netherlands, 1999.
(36) *SAINT, Program for Data Extraction and Reduction*; Bruker AXS, Inc.: Madison, WI, 2001.
(37) Sheldrick, G.M. *SHELXL-97, Program for Refinement of Crystal Structures*; University of Göttingen: Göttingen, Germany, 1997.
(38) Blatov, V.A.; O'Keeffe, M.; Proserpio, D.M. *CrystEngComm* **2010**, *12*, 44–48.
(39) O'Keeffe, M.; Peskov, M.A.; Ramsden, S.J.; Yaghi, O.M. *Acc. Chem. Res.* **2008**, *41*, 1782–1789.
(40) Blatov, V.A. *IUCr CompComm Newsletter* **2006**, *7*, 4, http://www.topos.ssu.samara.ru.
(41) Kahn, O. *Molecular Magnetism*; VCH Publishers, Inc.: New York, 1993.
(42) Manna, S.C.; Konar, S.; Zangrando, E.; Ribas, J.; Chaudhuri, N.R. *Polyhedron* **2007**, *26*, 2507–2516.
(43) Kahn, M.L.; Sutter, J.P.; Golhen, S.; Guionneau, P.; Ouahab, L.; Kahn, O.; Chasseau, D. *J. Am. Chem. Soc.* **2000**, *122*, 3413–3421.
(44) Tang, J.K.; Li, Y.Z.; Wang, Q.L.; Gao, E.Q.; Liao, D.Z.; Jiang, Z.H.; Yan, S.P.; Cheng, P.; Wang, L.F.; Wang, G.L. *Inorg. Chem.* **2002**, *41*, 2188–2192.
(45) Yue, Q.; Yang, J.; Li, G.H.; Li, G.D.; Xu, W.; Chen, J.S.; Wang, S.N. *Inorg. Chem.* **2005**, *44*, 5241–5246.